International Journal of Crashworthiness
Publication details, including instructions for authors and subscription information:
http://www.informaworld.com/smpp/title~content=t778188386

Improving the accuracy of vehicle crashworthiness response predictions using an ensemble of metamodels

Erdem Acar [a]; Kiran Solanki [b]
[a] Department of Mechanical Engineering, TOBB University of Economics and Technology, Sogutozu, Ankara, Turkey [b] Center for Advanced Vehicular Systems, Mississippi State University, Starkville, Mississippi, USA

Online Publication Date: 01 February 2009

To cite this Article Acar, Erdem and Solanki, Kiran(2009)'Improving the accuracy of vehicle crashworthiness response predictions using an ensemble of metamodels',International Journal of Crashworthiness,14:1,49 — 61
To link to this Article: DOI: 10.1080/13588260802462419
URL: http://dx.doi.org/10.1080/13588260802462419

International Journal of Crashworthiness
Vol. 14, No. 1, January 2009, 49–61

Taylor & Francis
Taylor & Francis Group

Improving the accuracy of vehicle crashworthiness response predictions using an ensemble of metamodels

Erdem Acar[a*] and Kiran Solanki[b]

[a]*Department of Mechanical Engineering, TOBB University of Economics and Technology, Sogutozu, Ankara, Turkey;* [b]*Center for Advanced Vehicular Systems, Mississippi State University, Starkville, Mississippi, USA*

(*Received 15 December 2007; final version received 4 September 2008*)

Due to the scale and computational complexity of current simulation codes for vehicle crashworthiness analysis, metamodels have become indispensable tools for exploring and understanding the design space. Traditional application of metamodelling techniques is based on constructing multiple types of metamodels based on a common data set, selecting the most accurate one and discarding the rest. However, this practice does not take full advantage of the resources devoted for constructing different metamodels. This drawback can be overcome by combining individual metamodels in the form of an ensemble. Two case studies with a high-fidelity finite element vehicle model subject to offset-frontal and side impact conditions are presented for demonstration. The prediction accuracies of the individual metamodels and the ensemble of metamodels are compared, and it is found for all the crash responses of interest that the ensemble of metamodels outperforms all individual metamodels. It is also found that as the number of metamodels included in the ensemble increases, the prediction accuracy of the ensemble of metamodels increases.

Keywords: metamodelling; ensemble; automobile; crashworthiness; side impact; offset-frontal impact; finite element analysis

Nomenclature

Err( )	the error metric that measures the accuracy of the ensemble of metamodels
FE	finite element
GMSE	generalised mean square cross-validation error
GP	Gaussian process
KR	Kriging
LHS	Latin hypercube sampling
NN	neural networks
N_M	number of metamodels
OFI	offset-frontal impact
PRS	polynomial response surface
RBF	radial basis function
R_1	intrusion distance in offset-frontal impact
R_2	intrusion distance in side impact
R_3	energy absorption in offset-frontal impact
R_4	energy absorption in side impact
SI	side impact
SLRSM	sequential linear response surface method
SVR	support vector regression
w_i	the weight factor the ith metamodel
$\hat{y}_i$	is the prediction of the ith metamodel
$\hat{y}_{\text{ens}}$	the prediction of the ensemble of metamodels

1. Introduction

Computer simulation codes for vehicle crashworthiness evaluation have contributed greatly to shortening the development periods for new vehicles with the advantages of numerical simulation techniques and computational capabilities. Designers of new vehicles must suggest a 'best design', which satisfies a variety of crash regulations along with other structural static and dynamic performance criteria. The main purpose of crashworthiness simulations is to evaluate structural performance and occupant injury criteria under various crash scenarios in the early stages of the design process. Even though modern parallel computing systems have made large-scale system-level simulations possible, high-fidelity crash simulations are still computationally expensive. For instance, a single crash analysis takes 15–20 hr utilising a high level of computational power [9]. Therefore, sensitivity analysis, design space exploration or optimisation studies, which requires repeated analyses, are computationally intractable.

Large computational expense of the high-fidelity analysis models led researchers to focus on various approximation methods that mimic the behaviour of the simulation model as closely as possible while being

*Corresponding author. Email: acar@etu.edu.tr

ISSN: 1358-8265

DOI: 10.1080/13588260802462419
http://www.informaworld.com

computationally more efficient to evaluate. These approximate models are known as metamodels or surrogate models. The most commonly used metamodelling techniques include polynomial response surface approximations (PRS) [21], multivariate adaptive regression splines [10], radial basis functions (RBF) [8,20], Kriging (KR) [19,25], Gaussian process (GP) [7,18], neural networks [27] and support vector regression (SVR) [4,13]. A recent and extensive review of metamodelling techniques in support of engineering design optimisation can be found in [31].

The accuracies of metamodels in predicting critical crash responses of an automobile have been investigated by many researchers. Yang *et al.* [32] evaluated different metamodels for crashworthiness safety optimisation and recommended the use of quadratic response surface approximations. Stander *et al.* [28] compared sequential linear response surface method (SLRSM), neural networks (NN) and Kriging (KR) for crashworthiness optimisation, and reported SLRSM as the most reliable one even with the deficiency of not being able to provide global approximations after the iterative optimisation. They also found NN to be slightly more stable than KR. Hamza and Saitou [14] evaluated the performances of RSA, RBF and NN for crashworthiness optimisation and reported RBF to be the most accurate. Fang *et al.* [9] compared several metamodelling methods for multi-objective crashworthiness optimisation and recommended the use of RBF. The evaluation of the use of metamodels in predicting the responses of crash simulations can also be found in the works of Gu [12], Horstemeyer *et al.* [15], Craig *et al.* [5] and Yang *et al.* [33]. As seen, different researchers found different types of metamodels performing the best for their problems. In general, it is difficult for an analyst to know which model is the best for a specific response for a specific crash scenario.

Traditional application of metamodelling techniques is based on constructing many different metamodels and then selecting the best one and discarding the rest. This practice has two major shortcomings. First, effort spent on constructing different metamodels is wasted. Second, since the performances of different metamodels are dependent on the training data set used, the selected metamodel is not guaranteed to be the optimal choice with the new data set. These drawbacks can be overcome by the use of an ensemble of metamodels rather than a single one. The resulting ensemble of metamodels takes advantage of the prediction ability of each individual metamodel to increase the accuracy of the predicted response [1,11,36].

To achieve high accuracy with limited number of finite element (FE) analyses, this paper utilises an ensemble of metamodels to estimate the crash performance of an automobile. The two main unique contributions presented in this paper are as follows: (a) The ensemble of metamodels is used for the first time to approximate the crash responses of a vehicle. (b) The effects of the prediction performances of individual metamodels on the performance of an ensemble are investigated. The number of individual metamodels in the ensemble is increased progressively to explore the evolution of the weights of individual metamodels as well as the error of the ensemble of metamodels.

The rest of the paper is organised as follows. Section 2 presents the concept of an ensemble of metamodels. Section 3 describes the automobile crash problem considered in the present paper. The results are presented and discussed in Section 4, followed by a summary of important conclusions provided in Section 5.

2. Ensemble of metamodels

The main premise behind the use of an ensemble of metamodels is to protect against the error and variability in the prediction of individual metamodels. The use of an ensemble of different models is first introduced by Bishop [2] and alternative formulations are proposed by Zerpa *et al.* [36], Goel *et al.* [11] and Acar and Rais-Rohani [1].

An ensemble is constructed by using a weighted average of different metamodels. The prediction of the ensemble of metamodels can be defined as

$$\hat{y}_{\text{ens}}(x) = \sum_{i=1}^{N_{\text{M}}} w_i(x)\hat{y}_i(x) \tag{1}$$

where $\hat{y}_{\text{ens}}$ is the prediction of the ensemble, N_M is the number of metamodels used, w_i is the weight factor for the ith metamodel and $\hat{y}_i$ is the prediction of the ith metamodel. The weighting factors satisfy

$$\sum_{i=1}^{N_M} w_i = 1 \tag{2}$$

Construction of an accurate ensemble requires judicious selection of the weight factors. The weight factors w_i for the metamodels need to be selected such that the prediction accuracy of the ensemble is maximised. Different weight selection procedures followed by different researchers are briefly discussed in the following paragraphs.

Zerpa *et al.* [36] proposed the use of a weighted average model of different metamodels (RS, KR and RBF) for the optimisation of an alkali surfactant–polymer flooding process. They chose the prediction variance as the error metric of their interest and set the value of the weight factor for each metamodel to be inversely proportional to the point-wise estimate of the prediction variance as

$$w_i = \frac{\frac{1}{V_i}}{\sum_{j=1}^{M} \frac{1}{V_j}} \tag{3}$$

where V_i is the prediction variance of the ith metamodel. The selection of weights via Equation (3) minimises the prediction variance of the weighted average model based on the assumption that the metamodel predictions are unbiased and uncorrelated, which is not always the case.

Goel *et al.* [11] considered an ensemble of three metamodels (RS, KR and RBF), used the generalised mean square cross-validation error (GMSE) of the individual metamodels and selected the weight factors as

$$w_i = \frac{w_i^*}{\sum_{j=1}^{M} w_j^*} \tag{4}$$

$$w_i^* = (E_i + \alpha \bar{E})^{\beta} \tag{5}$$

$$\bar{E} = \frac{1}{M} \sum_{i=1}^{M} E_i \tag{6}$$

where E_i is the GMSE of the ith metamodel calculated from

$$\text{GMSE} = \frac{1}{N} \sum_{k=1}^{N} \left(y^k - \hat{y}^{(k)}\right)^2 \tag{7}$$

where y^k is the true response at x_k and $\hat{y}^{(k)}$ is the corresponding predicted value from the metamodel constructed using all except the kth design point.

The parameters $\beta < 0$ and $\alpha < 1$ are selected by the analyst based on the importance of E_i and $\bar{E}$. According to Equations (4–6), a metamodel with a large GMSE shall have a small role in the ensemble by receiving a small weight factor and vice versa. Goel *et al.* [11] found $\alpha = 0.05$ and $\beta = -1$ lead to a good model in their study. Even though the analyst has flexibility in selecting the values of these parameters, the optimal values of these parameters may not be known beforehand.

Acar and Rais-Rohani [1] also used the GMSE as the error metric of interest and proposed that the weight factors of different metamodels can be selected via solving the following optimisation problem.

Table 1. Summary of FE models.

Item	Vehicle model	Barrier model	
		OFI	SI
Component	328	7	23
Node	320, 872	167, 182	232, 984
Shell element	546, 812	48, 640	54, 761
Solid element	30, 649	157, 520	192, 174
Beam element	63	0	0
Total mass (kg)	1210	128	1388

Find

$$w_i \tag{8}$$

Minimise

$$f = \text{Err}[\hat{y}_{\text{ens}}(w_i)] \tag{9}$$

such that

$$\sum_{i=1}^{N_M} w_i = 1 \tag{10}$$

where *Err*( ) is the error metric that measures the accuracy of the ensemble $\hat{y}_{\text{ens}}$. In this study, five different individual metamodels (i.e., PRS, RBF, KR, GP and SVR) are used in the ensemble. The weight factors of the individual metamodels are found by solving the optimisation problem stated in Equations (8–10). A brief summary of individual metamodelling techniques is provided in the appendix. In this paper, GMSE is used as the error metric of interest, while the other error metrics such as the prediction variance, correlation coefficient or coefficient of multiple determination can also be used as long as they are proven to be good surrogates for the actual error.

3. Automobile crash problem

3.1. Problem description

In safety design of automobiles, crashworthiness considerations are particularly important. An automobile is designed such that the impact energy in a possible crash scenario needs to be absorbed through structural deformation, while the intrusion distances of some structural elements must be smaller than their tolerable values. In this paper, two crash

Table 2. The description of the design variables and their initial (or baseline) values.

Input variable	Normalised variable	Component	Initial thickness (mm)
T_1	X_1	Left and right front doors	0.85
T_2	X_2	Left and right rear doors	0.83
T_3	X_3	Inner hood	0.65
T_4	X_4	Left and right outer B-pillars	1.61
T_5	X_5	Left and right middle B-pillar	0.71
T_6	X_6	Inner front bumper	1.96
T_7	X_7	Front floor panel	0.71
T_8	X_8	Left and right outer CBN	0.83
T_9	X_9	Left and right front fenders	1.52
T_{10}	X_{10}	Left and right inner front rails	1.90
T_{11}	X_{11}	Left and right outer front rails	1.52
T_{12}	X_{12}	Rear plate	0.71
T_{13}	X_{13}	Suspension frame	2.61

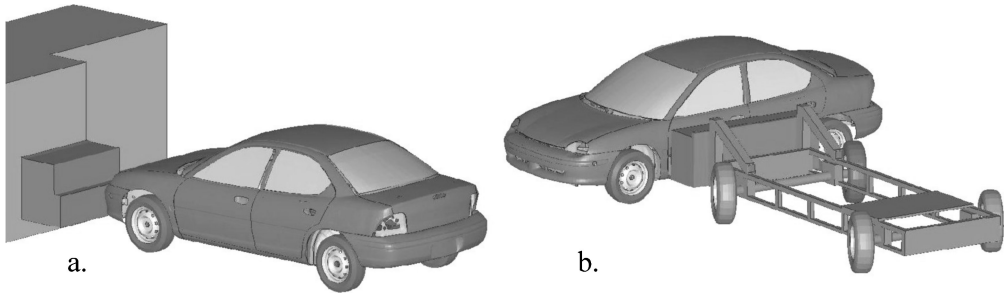

Figure 1. Full-scale FE models for impact simulations. (a) offset-frontal impact; (b) side impact.

scenarios are considered: (a) offset-frontal impact (OFI) and (b) side impact (SI), whereas other possible scenarios such as full-frontal impact, roof crush and rear impact are not included. In these two crash scenarios, the energy absorption and intrusion distances of structural elements are taken as critical responses. Thus, there exist four critical crash responses of interest: (1) the average intrusion distance of the front panel in OFI, (2) the average intrusion distance of the door in SI, (3) the total energy absorption of the vehicle at 40 ms in OFI and (4) the total energy absorption of the vehicle at 40 ms in SI.

In this study, a single full-scale FE model of a 1996 Dodge Neon is used in simulations of full frontal and side impacts. The model was originally developed at the U.S. National Crash Analysis Center [9,15,34,35]. The full-scale FE vehicle model used in this study has detailed meshes of 328 components that consist of 320,872 nodes and 577,524 elements. Approximately 95% of the elements were shell elements. The total vehicle mass is 1210 kg. This unified model is used in simulating two types of impacts, OFI in which the vehicle impacted a deformable barrier at 40% offset in the front and SI in which a moving deformable barrier impacted the vehicle from the side. In OFI, the deformable barrier model has 167,182 nodes and 206,160 elements with 76% being solid elements. The moving deformable barrier model in SI has a mass of 1388 kg and consists of 232,984 nodes and 246,935 elements with 78% being solid elements. Combining the FE models of the vehicle and deformable barriers, the model for OFI has a total of 488,054 nodes and 783,684 elements, and the model for

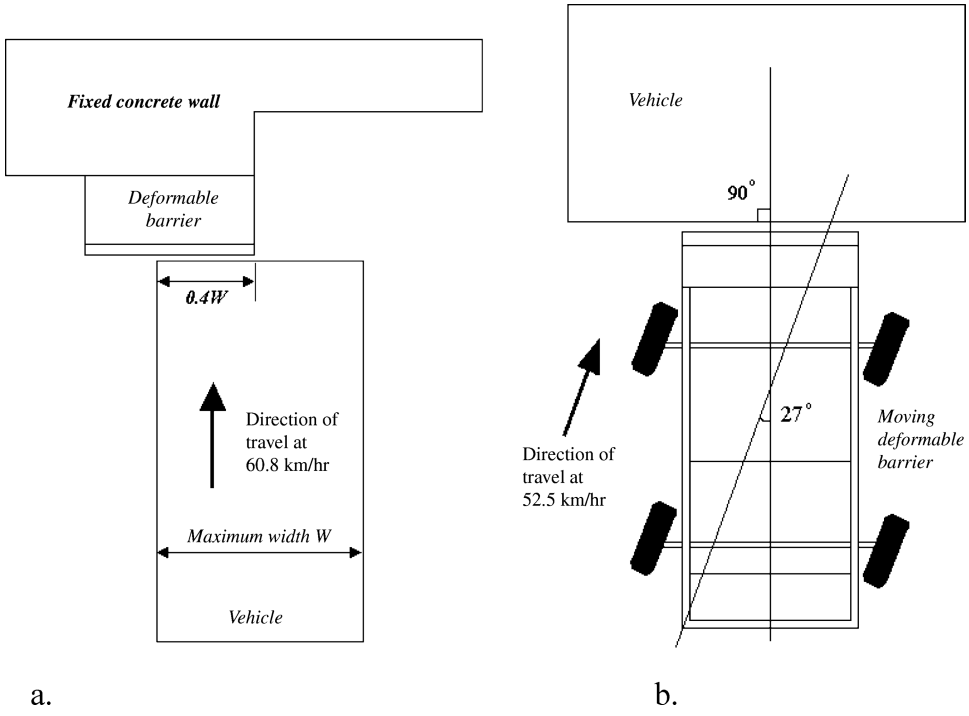

Figure 2. Plan view of test configurations (not drawn in scale). (a) offset-frontal impact; (b) side impact.

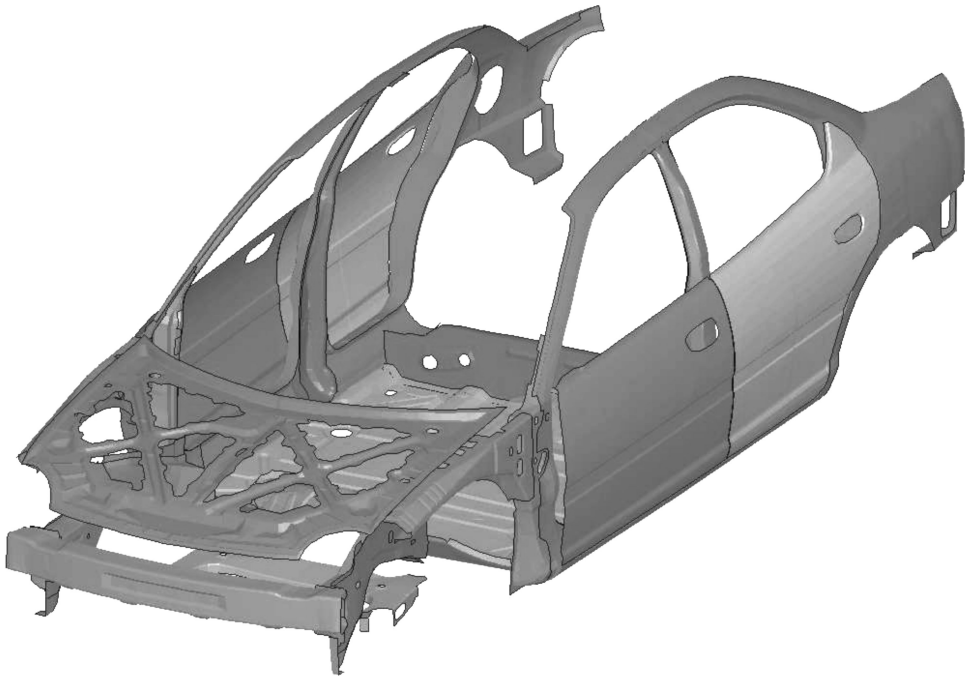

Figure 3. The components that have major influence on crash characteristics of the automobile.

Table 3. Design of experiments and critical responses.

No.	X_1	X_2	X_3	X_4	X_5	X_6	X_7	X_8	X_9	X_{10}	X_{11}	X_{12}	X_{13}	R_1	R_2	R_3	R_4
0	0	0	0	0	0	0	0	0	0	0	0	0	0	226	370	3.08	4.18
1	−1	−1	−1	−1	−1	−1	−1	−1	−1	−1	−1	−1	−1	164	385	3.13	3.79
2	−1	−1	−1	−1	0	0	0	0	0	0	0	0	0	135	370	3.05	4.22
3	−1	−1	−1	−1	1	1	1	1	1	1	1	1	1	87	355	2.90	4.05
4	−1	0	0	0	−1	−1	−1	0	0	0	1	1	1	247	383	2.99	3.87
5	−1	0	0	0	0	0	0	1	1	1	−1	−1	−1	80	364	3.02	3.98
6	−1	0	0	0	1	1	1	−1	−1	−1	0	0	0	145	378	3.03	3.81
7	−1	1	1	1	−1	−1	−1	1	1	1	0	0	0	224	366	2.97	3.95
8	−1	1	1	1	0	0	0	−1	−1	−1	1	1	1	201	384	3.24	3.75
9	−1	1	1	1	1	1	1	0	0	0	−1	−1	−1	227	364	3.02	3.92
10	0	−1	0	1	−1	0	1	−1	0	1	−1	0	1	244	376	3.02	3.82
11	0	−1	0	1	0	1	−1	0	1	−1	0	1	−1	239	362	3.05	3.93
12	0	−1	0	1	1	−1	0	1	−1	0	1	−1	0	186	337	3.01	4.08
13	0	0	1	−1	−1	0	1	0	1	−1	1	−1	0	231	375	3.23	3.95
14	0	0	1	−1	0	1	−1	1	−1	0	−1	0	1	227	361	2.99	4.04
15	0	0	1	−1	1	−1	0	−1	0	1	0	1	−1	260	376	2.97	3.87
16	0	1	−1	0	−1	0	1	1	−1	0	0	1	−1	193	365	3.05	4.31
17	0	1	−1	0	0	1	−1	−1	0	1	1	−1	0	251	378	2.88	3.82
18	0	1	−1	0	1	−1	0	0	1	−1	−1	0	1	235	357	3.16	3.95
19	1	−1	1	0	−1	1	0	−1	1	0	−1	1	0	242	371	3.01	3.85
20	1	−1	1	0	0	−1	1	0	−1	1	0	−1	1	207	354	2.98	4.02
21	1	−1	1	0	1	0	−1	1	0	−1	1	0	−1	204	340	3.22	4.41
22	1	0	−1	1	−1	1	0	0	−1	1	1	0	−1	163	367	2.88	3.95
23	1	0	−1	1	0	−1	1	1	0	−1	−1	1	0	198	345	3.20	4.07
24	1	0	−1	1	1	0	−1	−1	1	0	0	−1	1	263	365	3.08	3.84
25	1	1	0	−1	−1	1	0	1	0	−1	0	−1	1	224	361	3.05	4.07
26	1	1	0	−1	0	−1	1	−1	1	0	1	0	−1	229	373	3.00	3.92
27	1	1	0	−1	1	0	−1	0	−1	1	−1	1	0	207	355	3.02	4.29

Table 4. Actual values and ensemble of metamodel predictions of the responses.

	R_1 Intrusion OFI		R_2 Intrusion SI		R_3 Energy OFI		R_4 Energy SI	
	Act.	Pred.	Act.	Pred.	Act.	Pred.	Act.	Pred.
1	226	227.0	370	366.9	3.08	3.05	4.18	4.00
2	164	163.6	385	385.0	3.13	3.16	3.79	3.85
3	135	135.1	370	371.7	3.05	3.06	4.22	4.02
4	87	87.0	355	354.8	2.9	2.88	4.05	3.99
5	247	248.0	383	377.5	2.99	3.01	3.87	3.93
6	80	80.2	364	359.8	3.02	3.02	3.98	4.16
7	145	144.9	378	381.1	3.03	3.05	3.81	3.87
8	224	222.9	366	371.9	2.97	2.97	3.95	3.95
9	201	201.6	384	384.5	3.24	3.20	3.75	3.82
10	227	226.9	364	365.6	3.02	2.99	3.92	3.89
11	244	244.3	376	372.8	3.02	3.02	3.82	3.85
12	239	239.7	362	363.0	3.05	3.05	3.93	3.92
13	186	186.8	337	344.8	3.01	2.99	4.08	4.08
14	231	231.6	375	378.6	3.23	3.23	3.95	4.08
15	227	226.3	361	361.5	2.99	3.02	4.04	4.09
16	260	259.8	376	371.9	2.97	2.98	3.87	3.93
17	193	193.8	365	363.4	3.05	3.02	4.31	4.11
18	251	252.0	378	377.8	2.88	2.89	3.82	3.86
19	235	234.8	357	360.2	3.16	3.18	3.95	3.98
20	242	243.0	371	374.9	3.01	3.00	3.85	3.88
21	207	206.1	354	353.3	2.98	2.97	4.02	3.97
22	204	203.7	340	336.5	3.22	3.23	4.41	4.12
23	163	163.5	367	365.3	2.88	2.89	3.95	4.01
24	198	197.0	345	348.3	3.2	3.16	4.07	4.12
25	263	262.1	365	363.5	3.08	3.05	3.84	3.89
26	224	223.3	361	360.9	3.05	3.04	4.07	4.06
27	229	228.3	373	377.5	3	3.02	3.92	3.93
28	207	207.2	355	358.0	3.02	3.02	4.29	4.08
% error*	0.3		0.7		0.6		1.9	

*Mean absolute error is used as the error metric.

SI has 553,856 nodes and 824,459 elements. Details of the OFI and SI models are given in Table 1; the two FE models are illustrated in Figure 1.

A simulation of 100-ms OFI using LS-DYNA MPP v970 takes approximately 17 hr with 36 processors on an IBM Linux Cluster with Intel Pentium III 1.266 GHz processors and 607.5 GB RAM. A simulation of 100-ms SI takes approximately 29 hr with the same conditions as that of the OFI simulation. The initial speeds for OFI and SI are 60.8 km/hr and 52.5 km/hr, respectively. Figure 2 illustrates in detail the test configurations for OFI and SI.

3.2. Input variables for the metamodels

The input variables for the metamodels are the thicknesses of the components that have major influence on crash characteristics of the automobile (see Figure 3). The input variables, description of the components and the initial values of the design variables are provided in Table 2. Normalised values of the design variables X_i are used instead of the actual values of the design variables T_i to construct the metamodels, as this practice improves the accuracy of metamodels. The lower and upper bounds for the normalised variables are set to -1 and 1, respectively.

3.3. Design of experiments

Two main families of design of experiments exist [31]: (1) classic designs and (2) space filling designs. The most commonly used classic experimental designs include fractional factorial, central composite design and Box-Behnken designs [21]. Popular space filling designs include maximum entropy designs [6], minimax and maximin designs [16],

Table 5. Normalised GMSE of individual and ensemble of metamodels for different responses.

Response	PRS	RBF	KR	GP	SVR	ENS
R_1 (intrusion, OFI)	1.431	1.020	1.107	1.240	**1.0**	**0.918**
R_2 (intrusion, SI)	4.012	6.590	1.462	**1.0**	3.518	**0.938**
R_3 (energy, OFI)	6.491	9.547	4.745	**1.0**	4.759	**0.991**
R_4 (energy, SI)	6.066	2.535	1.481	1.224	**1.0**	**0.926**

Table 6. Weight factors of individual metamodels in the ensemble.

Response	PRS	RBF	KR	GP	SVR
R_1 (intrusion, OFI)	0.079	0.000	0.325	0.036	**0.560**
R_2 (intrusion, SI)	0.000	0.000	0.235	**0.763**	0.002
R_3 (energy, OFI)	0.002	0.000	0.000	**0.973**	0.025
R_4 (energy, SI)	0.021	0.000	0.000	0.294	**0.685**

Latin hypercube sampling (LHS) designs [22] and orthogonal arrays [29].

The main purpose of using a design of experiments method is to better represent the design space using a minimal set of design points. Taguchi orthogonal array L_{27} was used to generate the sampling points given in rows 1 to 27 and columns X_1 to X_{13} of Table 3. Recall that the descriptions of the responses in the last four columns of Table 3 were presented in Section 3.1.

4. Results

In this section, first the comparison of actual crash simulation results and cross-validation metamodel predictions for OFI and SI scenarios are presented. Then, the effects of using an ensemble of metamodels on the accuracy of predicting critical system responses are investigated. Finally, the effects of the performance of individual metamodels on the performance of the ensemble are explored.

4.1. *Comparison of actual simulations and metamodel predictions for OFI and SI*

Comparison of actual simulation results and cross-validation of an ensemble of metamodel predictions is provided in Table 4. It is found that the metamodels constructed for intrusion distances are more accurate than the metamodels constructed for the energy absorption. In addition, it is observed that the metamodels built for OFI responses are more accurate than those built for SI responses. The ensemble of metamodels constructed for energy absorption prediction under SI crash scenario resulted in the largest mean absolute cross-validation error. The magnitude of this error, '1.9%', is clearly acceptable for crash, which is a highly non-linear phenomenon.

Table 7. The change in the normalised GMSE for the intrusion distance in OFI (R_1) as the number of metamodels in the ensemble increases.

Metamodels included in the ensemble	SVR	SVR, RBF	SVR, RBF, KR	SVR, RBF, KR, GP	SVR, RBF, KR, GP, PRS
Normalised error	1	0.948	0.923	0.922	0.918

Table 8. Evolution of the weight factors of individual metamodels for the intrusion distance in OFI (R_1) as the number of metamodels in the ensemble increases.

Metamodels included in the ensemble	SVR	SVR, RBF	SVR, RBF, KR	SVR, RBF, KR, GP	SVR, RBF, KR, GP, PRS
Weight factors (in the same order as given in the first row)	1	0.542, 0.458	0.613, 0.000, 0.387	0.596, 0.000, 0.379, 0.025	0.560, 0.000, 0.325, 0.036, 0.079

4.2. *Improved accuracy by using the ensemble of metamodels*

The normalised error estimates for the four critical responses are listed in Table 5. Depending on the response of interest and the crash scenario, different individual metamodels outperform other metamodels. For instance, for intrusion distances, the SVR is the most accurate for OFI, while GP is the most accurate for SI. In the case of energies, on the other hand, GP outperforms the others for OFI, whereas SVR performs the best for SI. The dependency of the optimal metamodel on the response of interest and crash scenario indicates the necessity to examine multiple metamodels. The last column of Table 5 shows that the error of the ensemble of metamodels is smaller than the error of the best individual metamodel. For instance, the error of the ensemble was 8% smaller than the best individual metamodel for R_1. For R_3, on the other hand, Table 5 shows that the advantage of the ensemble over the best individual metamodel is the least apparent, because GP is far more superior than the other individual metamodels in the ensemble. The performance of the ensemble of metamodels is problem-dependent. Nevertheless, the error of the ensemble is smaller than those of the individual metamodels.

The weight factors of the individual metamodels in the ensemble for all the responses of interest are provided in Table 6. In general, the metamodels with smaller errors are assigned with larger weight factors to increase the prediction

Table 9. The change in the normalised GMSE for the intrusion distance in SI (R_2) as the number of metamodels in the ensemble increases.

Metamodels included in the ensemble	GP	GP, KR	GP, KR, SVR	GP, KR, SVR, PRS	GP, KR, SVR, PRS, RBF
Normalised error	1	0.938	0.938	0.938	0.938

Table 10. Evolution of the weight factors of individual metamodels for the intrusion distance in SI (R_2) as the number of metamodels in the ensemble increases.

Metamodels included in the ensemble	GP	GP, KR	GP KR, SVR	GP, KR, SVR, PRS	GP, KR, SVR, PRS, RBF
Weight factors (in the same order as given in the first row)	1	0.764, 0.236	0.763, 0.235, 0.002	0.763, 0.235, 0.002, 0.000	0.763, 0.235, 0.002, 0.000, 0.000

Table 12. Evolution of the weight factors of individual metamodels for the energy absorption in OFI (R_3) as the number of metamodels in the ensemble increases.

Metamodels included in the ensemble	GP	GP, KR	GP KR, SVR	GP, KR, SVR, PRS	GP, KR, SVR, PRS, RBF
Weight factors (in the same order as given in the first row)	1	0.997, 0.003	0.982, 0.002, 0.016	0.973, 0.000, 0.025, 0.002	0.973, 0.000, 0.025, 0.002, 0.000

accuracy of the ensemble. However, the relation between the errors and the weight factors is complex. For instance, even though RBF is the second most accurate model for R_1, the weight factor for RBF is zero. Similarly, although the errors of RBF and KR are much smaller than the error of PRS for R_4, the weight factor of PRS is larger than the weight factors of RBF and KR.

4.3. *The effect of performance of individual metamodels on the performance of the ensemble*

The results presented in the previous section show that by using an ensemble of metamodels with properly selected weight factors, the accuracy of response predictions can be improved. In this section, the effects of the performances of individual metamodels on the performance of the ensemble are investigated. One may argue that including inaccurate models in the ensemble may reduce the predictive capability of the ensemble. To question this argument, the ensemble is formed progressively by adding the metamodels one by one, starting from the most accurate metamodel to the worst accurate one. Table 7 shows that as the number of metamodels included in the ensemble increases, the error of the ensemble in predicting the intrusion distance in OFI, R_1, reduces. For R_1, the most accurate metamodel is SVR. By forming an ensemble of metamodels composed of SVR and the second most accurate metamodel, RBF, the error in R_1 prediction can be reduced by 5.2%. The addition of KR, GP and PRS into the ensemble further improves the prediction capability of the ensemble.

The evolution of the weight factors of the individual metamodels in the ensemble is presented in Table 8. As noted earlier, the general trend is that the metamodels with smaller errors are assigned with larger weight factors.

The variation of the normalised GMSE for intrusion distance in SI, R_2, is presented in Table 9. Recall that for R_2, the most accurate metamodel is GP. Table 9 shows that combining GP with the second most accurate metamodel, KR, reduces the error in R_2 prediction by 6.2%. The variation of error of the ensemble is different compared to the behaviour observed for R_1 (see Table 7) such that the addition of KR, GP and PRS to the ensemble does not have a significant effect on the error in R_2 prediction. The weight factors of the individual metamodels of the ensembles for R_2 estimation are provided in Table 10, which depicts that the weight factors for KR, GP and PRS are almost zero.

The variations of the normalised GMSE for absorbed energies in OFI and SI, R_3 andR_4, are presented in Tables 11 and 13, respectively. The general trend is the same: the addition of new members to the ensemble increases the accuracy of the ensemble. The weight factors of the individual metamodels of the ensembles for R_3 and R_4 are provided in Tables 12 and 14, respectively. In addition, the variations of the normalised error with the number of metamodels for all the responses are depicted in Figure 4.

Table 11. The change in the normalised GMSE for the energy absorption in OFI (R_3) as the number of metamodels in the ensemble increases.

Metamodels included in the ensemble	GP	GP, KR	GP, KR, SVR	GP, KR, SVR, PRS	GP, KR, SVR, PRS, RBF
Normalised error	1	0.999	0.994	0.991	0.991

Table 13. The change in the normalised GMSE for the energy absorption in SI (R_4) as the number of metamodels in the ensemble increases.

Metamodels included in the ensemble	SVR	SVR, GP	SVR, GP, KR	SVR, GP, KR, RBF	SVR, GP, KR, RBF, PRS
Normalised error	1	0.934	0.931	0.931	0.926

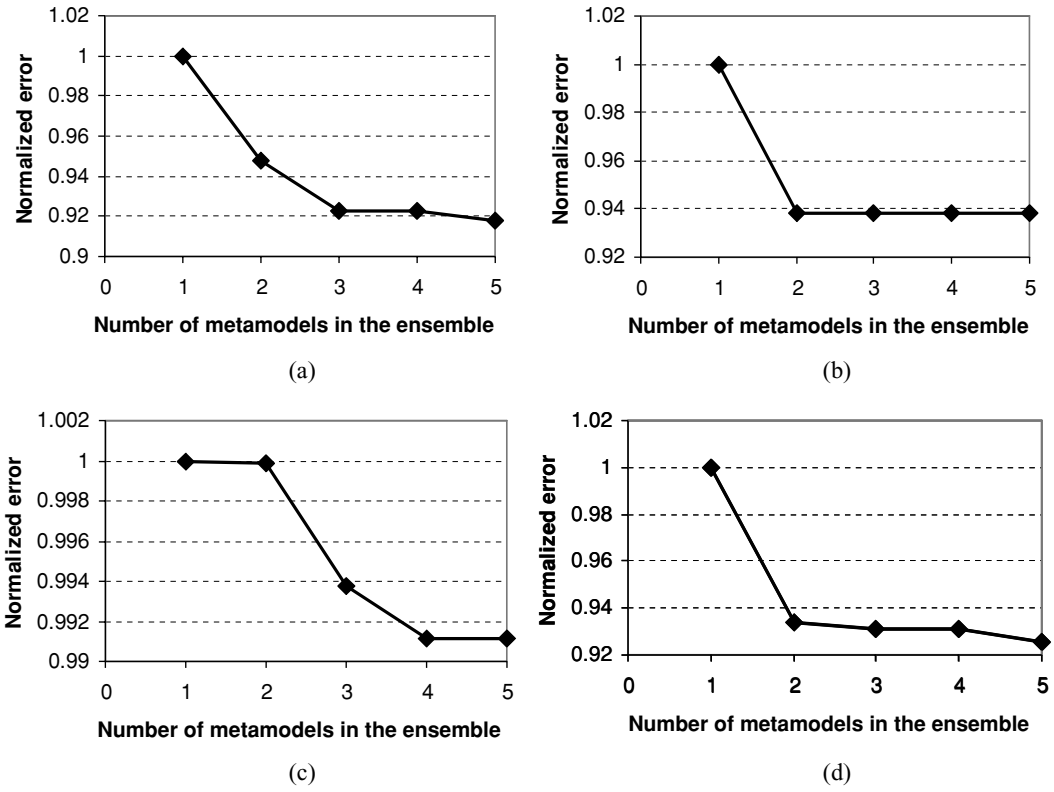

Figure 4. The variation of the normalised GMSE as the number of metamodels in the ensemble increases. (a) for R_1, (b) for R_2, (c) for R_3 and (d) for R_4.

Table 14. Evolution of the weight factors of individual metamodels for the energy absorption in SI (R_4) as the number of metamodels in the ensemble increases.

Metamodels included in the ensemble	SVR	SVR, GP	SVR, GP, KR	SVR, GP, KR RBF	SVR, GP, KR, RBF, PRS
Weight factors (in the same order as given in the first row)	1	0.689, 0.311	0.633, 0.308, 0.059	0.634, 0.307, 0.059, 0.002	0.685, 0.295, 0.000, 0.000, 0.021

5. Conclusions

This paper investigated the use of a weighted average ensemble of metamodels for improving the accuracy of automobile crash response approximations. The prediction capability of the ensemble of metamodels was compared to the best individual metamodel. In addition, the effects of the prediction performances of individual metamodels on the performance of ensemble were examined. From the results obtained in this study, the following points were observed:

- For all the crash responses considered, the ensemble of metamodels outperformed all individual metamodels such that the error of the ensemble was smaller than that of the most accurate individual metamodel.
- In general, the metamodels with smaller errors were assigned with larger weight factors to increase the prediction accuracy of the ensemble. However, the relation between the errors and the weight factors was complicated and in such a case an optimisation problem needs to be solved to attain the most accurate prediction.
- As the number of metamodels included in the ensemble increases, the prediction accuracy of the ensemble increases.
- If one of the individual metamodels is much more accurate than the other metamodels, the performance of the ensemble is dictated by that individual metamodel; hence constructing an ensemble of metamodels is not very advantageous.
- It is found that the metamodels constructed for intrusion distances are more accurate than the metamodels constructed for the energy absorption. In addition, it is observed that the metamodels built for OFI response predictions are more accurate than the metamodels built for SI response predictions.

Acknowledgments

This study is supported by the Center for Advanced Vehicular Systems, Mississippi State University and U.S. Department of Energy. The support of these institutions is greatly appreciated.

References

[1] E. Acar and M. Rais-Rohani, *Ensemble of metamodels with optimized weight factors*, Structural and Multidisciplinary Optimization (2008), published online, DOI: 10.1007/s00158–008-0230-y.

[2] C.M. Bishop, *Neural Networks for Pattern Recognition*, Oxford University Press Inc., New York, 1995, pp. 364–369.

[3] M. D. Buhmann, *Radial basis functions: theory and implementations*, Cambridge University Press, New York, 2003.

[4] S.M. Clarke, J.H. Griebsch, and T.W. Simpson, *Analysis of support vector regression for approximation of complex engineering analyses*, ASME J. Mech. Des. 127(11) (2005), pp. 1077–1087.

[5] K.J. Craig, N. Stander, D.A. Dooge, and S. Varadappa, *Automotive crashworthiness design using response surface-based variable screening and optimization*, Eng. Comput. 22(1) (2005), pp. 38–61.

[6] C. Currin, T.J. Mitchell, M.D. Morris, and D. Ylvisaker, *Bayesian prediction of deterministic functions, with applications to the design and analysis of computer experiments*, J. Am. Stat. Assoc. 86(416) (1991), pp. 953–963.

[7] D.D. Daberkow and D.N. Marvis, *An investigation of metamodeling techniques for complex systems design*, Proceedings of the 9th AIAA/ISSMO Symposium on Multidisciplinary Analysis and Optimization, Atlanta, GA, 2002.

[8] N. Dyn, D. Levin, and S. Rippa, *Numerical procedures for surface fitting of scattered data by Radial Basis Functions*, SIAM J. Sci. Stat. Comp. 7(2) (1986), pp. 639–659.

[9] H. Fang, K. Solanki, and M. Horstemeyer, *Numerical simulations of multiple vehicle crashes and multidisciplinary crashworthiness optimization*, Int. J. Crashworthiness 10(2) (2005), pp. 161–172.

[10] J.H. Friedman, *Multivariate adaptive regression splines*, Ann. Stat. 19(1) (1991), pp. 1–141.

[11] T. Goel, R.T. Haftka, W. Shyy, and N.V. Queipo, *Ensemble of surrogates*, Struct. Multidiscip. Optim. 33(3) (2007), pp. 199–216.

[12] L. Gu, *A Comparison of polynomial based regression models in vehicle safety analysis*, *ASME/DETC'01*, Pittsburgh, PA, 2001. Paper No. DETC2001/DAC-21063.

[13] S.R. Gunn, *Support vector machines for classification and regression*, Tech. Rep. Image Speech and Intelligent Systems Research Group, University of Southampton, UK, 1997.

[14] K. Hamza and K. Saitou, *Crashworthiness design using meta-models for approximating the response of structural members*, Proceeding of MDP-8, Cairo University Conference on Mechanical Design and Production, Cairo, Egypt, 2004, pp. 591–601.

[15] M. Horstemeyer, H. Fang, and K. Solanki, *Energy-based crashworthiness optimization for multiple vehicle impacts*, Transportation 2004: Transp. Environ. (2004) pp. 11–16.

[16] M.E. Johnson, L.M. Moore, and D. Ylvisaker, *Minimax and maximin distance designs*, J. Stat. Plan. Infer. 26(2) (1990), pp. 131–148.

[17] S.N. Lophaven, H.B. Nielsen and J. Søndergaard, *DACE - A MATLAB Kriging toolbox, informatics and mathematical modeling*, Technical University of Denmark, Lyngby, 2002.

[18] D.J.C. MacKay, *Introduction to Gaussian processes*, in *Neural Networks and Machine Learning*, C.M. Bishop, ed., Vol. 168 of NATO ASI Series, Springer, Berlin, 1998, pp. 133–165.

[19] J.D. Martin and T.W. Simpson, *Use of Kriging models to approximate deterministic computer models*, AIAA J. 43(4) (2005), pp. 853–863.

[20] A.A. Mullur and A. Messac, *Extended radial basis functions: More flexible and effective metamodeling*, Proceedings of the 10th AIAA/ISSMO Symposium on Multidisciplinary Analysis and Optimization, Albany, NY, 2004.

[21] R.H. Myers and D.C. Montgomery, *Response Surface Methodology: Process and Product Optimization Using Designed Experiments*, Wiley, New York, 2002.

[22] J.S. Park, *Optimal Latin-hypercube designs for computer experiments*, J. Stat. Plan. Infer. 39 (1994), pp. 95–111.

[23] M. Rais-Rohani, K. Solanki, and C. Eamon, *Reliability-based optimization of lightweight automotive structures for crashworthiness*, Proceedings of the 11th AIAA/ISSMO Multidisciplinary Analysis and Optimization Conference, AIAA Paper 2006–7004, Portsmouth, VA, 2006.

[24] C.E. Rasmussen and C.K.I. Williams, *Gaussian processes for machine learning*, MIT Press, Cambridge, 2006.

[25] J. Sacks, W.J. Welch, T.J. Mitchell, and H.P. Wynn, *Design and analysis of computer experiments*, Stat. Sci. 4(4) (1989), pp. 409–435.

[26] T.W. Simpson, T.M. Mauery, J.J. Korte, and F. Mistree, *Kriging models for global approximation in simulation-based multidisciplinary design optimization*, AIAA J. 39(12) (2001), pp. 2233–2241.

[27] M. Smith, *Neural Networks for Statistical Modeling*, Von Nostrand Reinhold, New York, 1993.

[28] N. Stander, W. Roux, M. Giger, M. Redhe, N. Fedorova, and J. Haarhoff, *A comparison of metamodeling techniques for crashworthiness optimization*, AIAA Paper No. 2004–4489, 10th AIAA/ISSMO Multidisciplinary Analysis and Optimization Conference, Albany, New York, 2004.

[29] G. Taguchi, Y. Yokoyama, and Y. Wu, *Taguchi Methods: Design of Experiments*, American Supplier Institute, Allen Park, MI, 1993.

[30] V. Vapnik, S. Golowich and A. Smola, *Support vector method for function approximation, regression estimation and signal processing*, M. Mozer, M. Jordan and T. Petsche, eds., Advances in Neural Information Processing Systems, MIT Press, Cambridge, 1997, pp. 281–287.

[31] G.G. Wang and S. Shan, *Review of metamodeling techniques in support of engineering design optimization*, ASME J. Mech. Des. 129(4) (2007), pp. 370–380.

[32] R.J. Yang, L. Gu, C. Gearhart, and C.H. Tho, *Approximations for safety optimization of large systems*, Proceedings of the ASME Design Engineering Technical Conferences, ASME Paper No. DETC2000/DAC-14245, Baltimore, MD, 2000.

[33] R.J. Yang, N. Wang, C.H. Tho, J.P. Bobineau, and B.P. Wang, *Metamodeling development for vehicle frontal impact simulation*, J. Mech. Des. 127(5) (2005), pp. 1014–1020.

[34] A.K. Zaouk, D. Marzougui, and N.E. Bedewi, *Development of a detailed vehicle finite element model, Part I: Methodology*, Int. J. Crash. 5(1) (2000), pp. 25–35.

[35] A.K. Zaouk, D. Marzougui, and C.D. Kan, *Development of a detailed vehicle finite element model, Part II: Material characterization and component testing*, Int. J. Crash. 5(1) (2000), pp. 37–50.
[36] L. Zerpa, N.V. Queipo, S. Pintos, and J. Salager, *An optimization methodology of alkaline-surfactant-polymer flooding processes using field scale numerical simulation and multiple surrogates*, J. Petrol. Sci. Eng. 47 (2005), pp. 197–208.

Appendix: Description of selected metamodelling techniques

In this appendix, a brief overview of the mathematical formulation of PRS, RBF, GP, KR and SVR metamodelling techniques is provided.

Polynomial response surface approximations (PRS)

The most commonly used PRS model is the second-order model in the form of a second-degree algebraic polynomial function as

$$\hat{f}(x) = b_0 + \sum_{i=1}^{L} b_i x_i + \sum_{i=1}^{L} b_{ii} x_i^2 + \sum_{i=1}^{L-1} \sum_{j=i+1}^{L} b_{ij} x_i x_j \qquad \text{(A1)}$$

where $\hat{f}$ is the response surface approximation of the actual response function f, L is the number of variables in the input vector $\boldsymbol{x}$ and b_0, b_i, b_{ii}, b_{ij} are the unknown coefficients to be determined by the least squares technique.

Radial basis function (RBF)

RBF methods were originally developed to approximate multivariate functions based on scattered data. For a data set consisting of the values of input variables and response values at n sampling points, the true function $f(\boldsymbol{x})$ can be approximated as

$$\tilde{f}(x) = \sum_{i=1}^{n} \lambda_i \phi(\|x - x_i\|) \qquad \text{(A2)}$$

where $\boldsymbol{x}$ is the vector of input variables, $\boldsymbol{x}_i$ is the vector of input variables at the ith sampling point, $\|\boldsymbol{x} - \boldsymbol{x}_i\| = \sqrt{(\boldsymbol{x} - \boldsymbol{x}_i)^{\mathrm{T}}(\boldsymbol{x} - \boldsymbol{x}_i)}$ is the Euclidean norm representing the radial distance r from design point $\boldsymbol{x}$ to the sampling point or centre $\boldsymbol{x}_i$, ϕ is a radially symmetric basis function and $\lambda_i, i = 1, n$ are the unknown interpolation coefficients. Equation (A2) represents a linear combination of a finite number of radially symmetric basis functions. Some of the most commonly used RBF formulations include $\phi(r) = r^2 \log(r)$ (thin-plate spline); $\phi(r) = e^{-\alpha r^2}$, $\alpha > 0$ (Gaussian); $\phi(r) = \sqrt{r^2 + c^2}$(multi-quadric); and $\phi(r) = 1/\sqrt{r^2 + c^2}$ (inverse multi-quadric). The parameter c in the multi-quadrics is a constant. If the r values are normalised to the range of (0,1), then $0 < c \leq 1$. The choice of $c = 1$ is found to be suitable for most function approximations. The feature that makes these functions excellent candidates for ϕ is not simply their radial symmetry but their smoothness and certain properties of their Fourier transform (Buhmann, 2003)[3]. In this study, we have chosen the multiquadric formulation of RBF because of its prediction accuracy and commonly linear and possibly exponential rate of convergence with increased sampling points.

Given the design coordinates of n sampling points and associated responses, the unknown coefficients in Equation (A2) are found by minimising the residual or the sum of the squares of the deviations expressed as

$$R = \sum_{j=1}^{n} \left[f(\boldsymbol{x}_j) - \sum_{i=1}^{n} \lambda_i \phi(\|\boldsymbol{x}_j - \boldsymbol{x}_i\|) \right]^2 \qquad \text{(A3)}$$

Expressed in matrix form, Equation (A3) appears as

$$[A]\{\boldsymbol{\lambda}\} = \{\boldsymbol{f}\} \qquad \text{(A4)}$$

where $[A] = [\phi\|\boldsymbol{x}_j - \boldsymbol{x}_i\|], \quad j = 1, n;\ i = 1, n, \quad \{\boldsymbol{\lambda}\}^{\mathrm{T}} = \{\lambda_1, \lambda_2, ..., \lambda_n\}^{\mathrm{T}}$ and $\{\boldsymbol{f}\}^{\mathrm{T}} = \{f(x_1), f(x_2), ..., f(x_n)\}^{\mathrm{T}}$. The coefficient vector λ is obtained by solving Equation (A4).

Gaussian process (GP)

Gaussian process assumes that the output variables $f_N = \{f_n(x_n^1, x_n^2, \mathbf{K}, x_n^L)\}_{n=1}^{N}$ are related to each other with a Gaussian joint probability distribution

$$P(f_N|C_N, X_N) \qquad \text{(A5)}$$
$$\frac{1}{\sqrt{(2\pi)^N |C_N|}} \exp\left[-\frac{1}{2}(f_N - \mu)^{\mathrm{T}} C_N^{-1} (f_N - \mu) \right]$$

where $X_N = \{x_n\}_{n=1}^{N}$ are N pairs of L-dimensional input variables $x_n = (x_n^1, x_n^2, \mathbf{K}, x_n^L)$, C_N is the covariance matrix with elements of $C_{ij} = C(x_i, x_j)$ and μ is the mean output vector. GP estimates the output at a prediction point $\boldsymbol{x}_p = (\boldsymbol{x}_p^1, \boldsymbol{x}_p^2, \mathbf{K}, x_p^L)$ as

$$\hat{f}(\boldsymbol{x}_p) = k^{\mathrm{T}} C_N^{-1} f_N \qquad \text{(A6)}$$

where $k = [C(\boldsymbol{x}_1, \boldsymbol{x}_p), \mathbf{K}, C(x_N, x_p)]$. One of the nice properties of the GP is that the standard deviation at the prediction point is readily available without a requirement of any extra simulations. This standard deviation can be utilised as an error measure and can be calculated from

$$\sigma_{\hat{f}(\boldsymbol{x}_p)} = \kappa - k^{\mathrm{T}} C_N^{-1} k \qquad \text{(A7)}$$

where $\kappa = C(x_p, x_p)$.

We notice from Equation (A6) that the GP prediction depends on the covariance matrix C_N. The elements of this matrix are calculated from

$$C_{ij} = \theta_1 \exp\left[-\frac{1}{2} \sum_{l=1}^{L} \frac{\left(x_i^{(l)} - x_j^{(l)}\right)^2}{r_l^2} \right] + \theta_2 \qquad \text{(A8)}$$

$$C_{ij} = \theta_1 \exp\left[-\frac{1}{2} \sum_{l=1}^{L} \frac{\left(x_i^{(l)} - x_j^{(l)}\right)^2}{r_l^2} \right] + \theta_2 + \delta_{ij}\theta_3 \qquad \text{(A9)}$$

where $\theta_1, \theta_2, \theta_3$ and r_l ($l = 1, 2, \ldots, L$) are called 'hyperparameters'. Here δ_{ij} is the Kronecker delta and θ_3 is an independent noise parameter. The hyperparameters are selected so as to maximise the logarithmic likelihood that the model prediction matches the training response data. The logarithmic likelihood function L is given in Equation (A10).

$$L = -\frac{1}{2}\log|C_N| - \frac{1}{2}f_N^{\mathrm{T}}C_N^{-1}f_N - \frac{N}{2}\log 2\pi + \ln P(\theta) \tag{A10}$$

where $P(\theta)$ is the prior distribution of the hyperparameters. In most of the applications, there is no prior knowledge of the values of the hyperparameters, so the prior distribution is uniform. Then the last term of Equation (A10), $\ln P(\theta)$, is a constant and can be taken as zero for the purpose of optimisation, as we did in this work.

The covariance function given in Equation (A8) defines the interpolation mode of the GP metamodel that passes exactly through all the training data points. On the other hand, Equation (A9) defines the regression mode of the model, which allows us to build smoother surfaces for problems with noisy data.

With the noise of the output values filtered out, the predicted surface becomes less complex and may not pass through all the training points; however, it provides a better prediction at the non-training points. In this work, we used Gaussian process code from Rasmussen and Williams (2006)[24].

Kriging (KR)

The basic assumption of KR is the estimation of the response in the form

$$f(x) = p(x) + Z(x) \tag{A11}$$

where f is the response function of interest, p is a known polynomial that globally approximates the response and $Z(x)$ is the stochastic component that generates deviations such that the KR model interpolates the sampled response data. The stochastic component has a mean value of zero and covariance of

$$COV[Z(x_i), Z(x_j)] = \sigma^2\mathbf{R}[R(x_i, x_j)] \tag{A12}$$

where $\mathbf{R}$ is $N \times N$ correlation matrix if N is the number of data points, $R(x_i, x_j)$ is the correlation function between the two data points x_i and x_j. Mostly, the correlation function is chosen as Gaussian, that is,

$$R(\theta) = \prod_{k=1}^{L}\exp\left(-\theta_k d_k^2\right) \tag{A13}$$

where L is the number of variables, $d_k = x_k^i - x_k^j$ is the distance between the kth components of the two data points x_i and $x_j$and θ_k are the unknown parameters to be determined.

Once the correlation function has been selected, the response f is predicted as

$$\hat{f}(x) = \hat{\beta} + \mathbf{r}^{\mathrm{T}}(x)\mathbf{R}^{-1}(f - \hat{\beta}\,\boldsymbol{p}) \tag{A14}$$

where $\mathbf{r^T}(x)$ is the correlation vector of length N between a prediction point x and the N sampling points, f represents the responses at the N points and $\boldsymbol{p}$ is an L-vector of ones (in the case $p(x)$ is taken as a constant). The vector $\boldsymbol{r}$ and scalar $\hat{\beta}$ are given by

$$\begin{aligned}\mathbf{r}^{\mathrm{T}}(x) &= [R(x, x^1), R(x, x^2), \mathbf{K}, R(x, x^N)]^{\mathrm{T}}, \hat{\beta} \\ &= (\boldsymbol{p}^{\mathrm{T}}\boldsymbol{R}^{-1}\boldsymbol{p})^{-1}\boldsymbol{p}^{\mathrm{T}}\boldsymbol{R}^{-1}\mathrm{f}\end{aligned} \tag{A15}$$

The variance of the output model (which is different from the variance of the sampled output) can be estimated as

$$\hat{\sigma}^2 = \frac{(f - \hat{\beta}\,\boldsymbol{p})^{\mathrm{T}}\boldsymbol{R}^{-1}(f - \hat{\beta}\,\boldsymbol{p})}{N} \tag{A16}$$

The unknown parameters θ_k can be estimated by solving the following constrained maximisation problem (Simpson *et al.* 2001[26])

$$\begin{aligned}&Max\ \Phi(\Theta) = \frac{-\left[N\ln(\hat{\sigma}^2) + \ln|\mathbf{R}|\right]}{2} \\ &s.t.\quad \Theta > 0\end{aligned} \tag{A17}$$

where $\boldsymbol{\Theta}$ is the vector of unknown parameters θ_k, and both $\hat{\sigma}$ and $\mathbf{R}$ are functions of $\boldsymbol{\Theta}$.

In this work, we use a MATLAB Kriging toolbox developed by Lophaven *et al.* (2002)[17].

Support vector regression (SVR)

The prediction via SVR can be performed through linear or nonlinear regression. When linear regression is performed, then the function is predicted as

$$\hat{f}(x) = \langle w \cdot x\rangle + b \tag{A18}$$

where $\langle w \cdot x\rangle$ is the dot product of w and x. We would like to have the approximation function as flat as possible. For that purpose, we solve the following optimisation problem:

$$\begin{aligned}&Min\ \ \tfrac{1}{2}|w|^2 \\ &s.t.\ \ y_i - \langle w \cdot x_i\rangle - b \le \varepsilon \\ &\qquad \langle w \cdot x_i\rangle + b - y_i \le \varepsilon\end{aligned} \tag{A19}$$

This formulation assumes that the function $\hat{f}(x)$ can approximate all the y_i training points within an ε precision. However, this may not be true for all training points and two slack variables can be introduced to yield a modified formulation (Vapnik *et al.* 1997)[30]. Now, the optimisation problem is

$$\begin{aligned}&Min\ \ \tfrac{1}{2}|w|^2 + C\sum_{i=1}^{l}\xi_i + \xi_i^* \\ &s.t.\ \ y_i - \langle w \cdot x_i\rangle - b \le \varepsilon + \xi_i \\ &\qquad \langle w \cdot x_i\rangle + b - y_i \le \varepsilon + \xi_i^* \\ &\qquad \xi_i, \xi_i^* \ge 0\end{aligned} \tag{A20}$$

where C determines the tradeoff between the flatness and tolerance. The second term in the objective function is referred to as ε-insensitive loss function (Vapnik *et al.* 1997)[30]. If we write the Lagrangian function, assess the Karush-Kuhn-Tucker (KKT) conditions and substitute KKT conditions into the Lagrangian function, we can write the optimisation problem in dual

form as

$$\begin{aligned} Max \quad & -\frac{1}{2}\sum_{i},\, j = 1^{l}(\alpha_i - \alpha_i^*)(\alpha_j - \alpha_j^*)\langle x_i \cdot x_j\rangle \\ & -\varepsilon \sum_{i} = 1^{l}(\alpha_i - \alpha_i^*) + \sum_{i=1}^{l} y_i(\alpha_i - \alpha_i^*) \\ s.t. \quad & \sum_{i=1}^{l}(\alpha_i - \alpha_i^*) = 0 \\ & (\alpha_i - \alpha_i^*) \in [0, C] \end{aligned} \tag{A21}$$

The weights and the linear regression are then calculated through

$$w = \sum_{i=1}^{l}(\alpha_i - \alpha_i^*)x_i,\ \hat{f}(x) = \sum_{i=1}^{l}(\alpha_i - \alpha_i^*)\langle x_i \cdot x_j\rangle + b \tag{A22}$$

Instead of using linear regression, non-linear regression can also be used by replacing the dot product of the input vectors with kernel functions. Commonly used Kernel functions include non-linear polynomials, Gaussian and Sigmoid kernel functions. In this case, the optimisation function is written as

$$\begin{aligned} Max \quad & -\frac{1}{2}\sum_{i},\, j = 1^{l}(\alpha_i - \alpha_i^*)(\alpha_j - \alpha_j^*)k(x_i \cdot x_j) \\ & -\varepsilon \sum_{i=1}^{l}(\alpha_i - \alpha_i^*) + \sum_{i=1}^{l} y_i(\alpha_i - \alpha_i^*) \\ s.t. \quad & \sum_{i=1}^{l}(\alpha_i - \alpha_i^*) = 0 \\ & (\alpha_i - \alpha_i^*) \in [0, C] \end{aligned} \tag{A23}$$

Then, the support vector regression approximation is obtained through

$$\hat{f}(x) = \sum_{i=1}^{l}(\alpha_i - \alpha_i^*)k(x_i \cdot x_j) + b \tag{A24}$$

More detailed information can be found in [4]. In this work, we used the MATLAB code developed by Gunn [13].